Wastewater Treatment Using Cellulose Nanofiber (CNF)-Based Green Filters: A Sustainable Approach to Water Purification

M.M.Alam[1*], Md. Johurul Islam[2], Sumsun Naher[3*], Kenneth TV Grattan[3], S. Narjim[4] and Claire Heffernan[5]

*Corresponding authors

[1] *Department of Electrical and Electronic Engineering, Islamic University, Kushtia, ~~Bangladesh;~~Bangladesh.*
email: malam@eee.iu.ac.bd
[2] *Department of Physics, Bangladesh University of Engineering and Technology (BUET), Dhaka-1000, Bangladesh; email: Johurul.eee.iu@gmail.com*
[*3]*Department of Engineering, City St. George's, University of London, UK, E-mail: Sumsun.Naher.1@citystgeorges.ac.uk*
[3] *Department of Engineering, City St. George's, University of London, UK, E-mail: ~~K.T.V.Grattan@city.ac.uk~~K.T.V.Grattan@citystgeorges.ac.uk*
[4] *Department of Electrical and Electronic Engineering, Pabna University of Science and Technology, Pabna, Bangladesh; email: sadi.narjim@gmail.com*
[5] *London International Development Centre, London, UK, E-mail: Claire.Heffernan@lidc.ac.uk*

Abstract:

Nanocellulose (NC), as a material, is attracting considerable attention due to its renewable nature, anisotropic shape, excellent mechanical properties, good biocompatibility, tailorable surface chemistry and interesting optical properties. In addition is it easy to source in many developing countries and is inexpensive, as it is often simply considered as a waste product from banana production. In this study, banana fibers (BFs) are chemically modified and converted into Cellulose NanoFibers (CNFs), for incorporation into water filters. The properties of the CNFs thus created were then characterized by using several analytical techniques, such as scanning electron microscopy (SEM), Fourier Transform Infra-Red (FTIR) spectroscopy, X-ray diffraction (XRD) and a thermal study, to understand them better and thus optimize their properties. The aim in so doing is for the CNFs to be used as the basis for fabricating an innovative and inexpensive design of filter, for water purification, and which can be used locally. The key purpose of the work has been the development of a CNF-based water filter, which was fabricated by using a mixture of locally-sourced kaolin (Bijoypur clay) and CNFs, in a 10:1 weight ratio. The water filters thus fabricated were tested and their performance evaluated by exposure to simulated wastewater, containing a combination of six readily available antibiotics (Ciprofloxacin, Clarithromycin, Erythromycin, Metronidazole, Sulfamethoxazole and Trimethoprim). This evaluation was enabled by using UV-Visible spectroscopy measurements, before and after filtration. These simple, CNF-based water filters were found to be highly effective in removing the antibiotic solution used on each pass through the filter, showing a figure of merit of 2.7 ± 0.1 per pass. This approach to filter production provides a simple, inexpensive environmentally friendly and locally-sourced

Formatted: Font: (Default) Calibri, 11 pt
Formatted: List Paragraph
Field Code Changed
Formatted: English (United Kingdom)
Formatted: Font: (Default) Calibri, 11 pt, Not Italic

solution to the reduction of antibiotics in wastewater, reducing the pollution problems those antibiotics entering the wastewater supply causes.

Keywords: Banana fiber, Cellulose Nano Fiber, Antibiotics, Biodegradable, and CNF based water filter, Bijoypur clay

1. Introduction

Antibiotics are of particular importance and widely used in a number of fields, such as human therapy, veterinary medicine and as growth promoters. However, waste from numerous sources where antibiotics accumulate, such as in sewage treatment plants and animal feeding operations are problematic and as most antibiotics are poorly absorbed by humans and animals, with about 25% to 75% leaving the organisms via feces or urine (Chee-Sanford et al., 2001). A major concern with antibiotic residues in the environment is the inducement of resistance in bacterial strains. Thus recent reports on antibiotic detection in various wastewater sources continue to raise such environmental concerns, especially in developing countries where various antibiotics are often bought 'over the counter' and without prescription. In addition to obtaining a better understanding of the transport pathways and the environmental destination of antibiotics, efforts must be made at local level to deal systematically with effluents from wastewater treatment, including when containing antibiotic residue (Wang et al. 2018). Studies focusing exclusively on the occurrence of antibiotics in various wastewater treatment systems are somewhat limited: data from Europe is more available than that from developing countries. As over the past few years, antibiotics have been considered as pollutants due to their continuous input and persistence in the aquatic ecosystems (even at low concentrations), and to prevent such contamination, processes to degrade/remove antibiotics are needed – and these must be cost-effective. Various studies have looked at conventional remediation techniques (e.g. biological processes, filtration, coagulation, flocculation and sedimentation), advanced oxidation processes (AOPs), adsorption, membrane processes and thus a wide range of individual and combined methods have been reported (GilPavas et al., 2017; Teh et al 2016; Drinan, 2001). However, for use in developing countries, cost is a key factor and thus in this work a simple to implement, low-cost solution using locally available and easy to process materials has been discussed. Thus the worldwide problem of their ineffective removal from water and wastewater using *conventional* treatment methods can be tackled in a way appropriate to the developing world using locally-available materials and filtration designs.

This work tackles the above problem through the development of a simple, inexpensive filter based on the use of cellulose-based materials where in recent years, research on the extraction and wider exploration of the uses of various cellulose-based materials has been increasing rapidly. Nano cellulose (NC) has been shown to be one of the most widely available 'green' materials, due to its excellent characteristics such as high aspect ratio, good mechanical properties, renewability and biocompatibility (Wan et al. 2021). The hydroxyl functional groups permit an extensive array of functionalizations of the material via chemical reactions, which allows the development of various materials with a variety of important features (Hokkanen et al. 2016, Trache et al., 2001). Different biodegradable polymers, such as banana

fiber (BF), coconut coir, jute, bamboo etc. have been used for the preparation of NC, and thus ultimately to prepare nanocomposites for use in a variety of applications.

Thus the main purpose of this research is to design a simple to implement, yet effective and minimal cost antibiotic filter. To do so the research has focused on extracting nanofibers from natural available biopolymers (in one developing country where the problem is acute and the solution proposed can be applied – in Bangladesh) and thus to enhance the fiber properties so that the solution offered finds applications as an advanced product, to satisfy the technological demands of the next generation. Thus with ease of use and minimal cost as key factors in the work, an approach is proposed and developed in this work to produce cheap adsorbents for wastewater treatment from locally available materials, such as NC and clay materials.

To design and implement a water filter which is eco-friendly and cost-effective for water treatment, NC are employed in this work as a reinforcing element in a base of china clay (kaolin). Kaolin has been chosen for its ready availability and low cost, and as it is contains chemicals such as aluminum, silver, silicon material, essential for treatment of germs (Deer et al., 1992, Hani...2024 and An et al..,2024). For the adsorption of heavy metals, kaolin clay is known to be a promising material (Gupta et al., 2008). However, natural fibers, because of their low cost, abundance, biocompatibility and biodegradability, are very promising materials for replacing the synthetic ones (Islam et al., 2020), which are more expensive and less available, in such filters. Hence, a wide variety of different natural fibers including banana tree fibers (BF) are being considered as here reinforcements in the fabrication of composites (Islam et al., 2021). BF is ideal to use in this way as it is biodegradable and has a low density with good specific mechanical properties. However, a major advantage for this application is that it can be utilized as a source of cellulose for producing nanocellulose (NC) (Sharma et al..,2024 and Radoor et al..,2024).

We hypothesize that cellulose nanofibers (CNFs) extracted from banana fibers and combined with locally available kaolin clay can create an effective, biodegradable, and low-cost water filtration system capable of removing antibiotic residues from wastewater. This system is predicted to achieve over 90% filtration efficiency by leveraging the high adsorption capacity of CNFs and the antimicrobial properties of kaolin.

In this work the focus is on the design, development and evaluation of a low-cost antibiotic filter for wastewater: thus, recent advances in the preparation, modification, and emerging application of CNFs, especially NC extracted from BF, are described and their use in such a filter discussed, based on the different characterization and analysis methods (Lakretz et al. 2014). Thus such NC in different compositions were used to make water filter for water purification and the work reported in this paper presents preliminary results on the effectiveness of the preparation and testing of filters based on such designs, with consideration of the future research directions for their production.

2. Experimental

2.1. CNF preparation

In this section, the processes of CNF preparation from the raw banana plant material are described and the issues involved discussed.

2.1.1 Materials

Banana bast fibre comes from the banana plant (*Musa paradisiaca)*, which normally is a waste product after the fruit is collected. After natural fermentation of the banana plant (by immersion in water), it becomes banana bast fiber. Such banana bast fibre is the raw material for the nanocellulose used in this work and to create it (using locally sourced or readily available materials), 10% soap solution was collected from local market (Dhaka, Bangladesh), together with Sodium Hydroxide (NaOH – purity 98%), Sodium hypo-Chlorite (NaOCl – purity 80%), Sodium acetate (CH_3COONa – purity 98%), Glacial acetic acid (CH_3COOH – purity 100%), Sodium meta-bi-sulphite ($Na_2S_2O_5$ – purity 99.9%), and Sulfuric acid (H_2SO_4 – purity 98%) from E. Marck KG, Germany.

2.1.2 Methods

2.1.2.1. Collection and Preparation of Banana Fiber

The banana (*Musa sapientum*) fiber, from different species, is found widely in the various regions, in this case in Bangladesh (Imam & Akter, 2011), but here the banana fiber used was collected from Khulna, Bangladesh. The mature banana plants attain a height of ~5m, after which they are cut down and tied up in bundles, then 'retted' in dirty water for 15 to 20 days (where retting is the process of rotting away the inner stalk using bacteria, leaving the outer fibers intact – the fiber was then separated from reinforcing and sticky materials). The fiber then was washed in clean water several times and dried in air without exposing it to sunlight. Finally, the fiber was dried in an electric oven at 100°C and stored in a desiccator (Percot et al., 2003).

2.1.2.2 Scouring of Banana Fiber

Waste agricultural fiber, such as is used here, contains impurities such as dirty materials and fatty, waxy and gummy substances. Scouring is the process to remove those impurities from the biodegradable fiber (Mateo et al., 2021). To do so, soda and detergent, as a surface-active agent, is used for scouring. In this process, first the banana fibers are cut to a length of 30 cm and a solution of 6 g Na_2CO_3 with 4 g detergent is made up in a large beaker – this is then left for 2 h (at a temperature of 60 ºC) with the fibers and solution in a ratio ~1:30. Finally, the fibers were washed several times with distilled water and dried in an electric oven at 100 ºC for 30 minutes, than stored in a desiccator.

2.1.2.3 Alkali Treatment

Alkali treatment is known to improve the fiber mechanical properties (Herbert et al. 1954). In this study, using banana fiber, 5% w/v NaOH solution was added (as >5% NaOH can cause fiber damage and reduce its mechanical strength (Mahjoub et al. 2014) and the fibers were immersed for ~2 hours, at 40°C with continuous stirring being maintained. This treated fiber

is termed alpha-cellulose (and the filter solution will contain hemi-cellulose and lignin). Fig. 1 shows the effect of the alkali treatment of these banana fibers. Next, this alpha-cellulose will be bleached.

2.1.2.4 Bleaching

To bleach the dried banana fibers, at 90ºC temperature, 4% w/v (or 20 gpl solution) of NaOCl was used (with pH 10.5 at room temperature). This buffer mixture was used to reduce the pH of solution to 4.0 and was prepared by mixing acetic acid, sodium acetate and distilled water in the ratio of 10ml: 10g: 100ml. With the help of a buffer solution dropper, the NaOCl solution was slowly dissolved and the solution stirred. When the pH reached 4.0, the alpha-cellulose fibers were immersed in the solution and the stirring continued, at 85 ºC. After 2 hours, the solution was filtered, the fibers washed with distilled water and dried at room temperature. This bleaching treatment was repeated – a 'double bleaching' of fiber was carried out and after thorough washing, the fiber dried at room temperature and stored in the desiccator. Fig. 1 shows the bleached banana fibers.

2.1.2.5 Cellulose Nano Fiber (CNF)

The bleached cellulose fibers were cut into as small samples as possible by using scissors. The cellulose nano fiber was formed by double acid hydrolysis in which H_2SO_4 solution (~60 wt %) was stirred for 2 hours at 40°C temperature on a magnetic hot plate. The ratio of fiber to liquor was 1:15 (15 ml of sulfuric acid to 1g cellulose). After 1 hour, 50ml of ice was added to stop hydrolysis. After stirring for a further 30 minutes, the solution was centrifuged at room temperature, after which the CNF created was washed with distilled water, until a pH of 6.5 was recorded. Finally, the CNF was prepared and stored in ethanol (Rahman et al., 2018) and Fig. 1 shows a series of photographs illustrating the process and finally the extracted CNF from the banana fibers.

Fig.1: Photographs of the sequence of the stages of preparation of cellulose nano fiber (CNF)

2.2 Kaolin (Bijoypur clay):

The kaolin used in this work was collected locally (from the Bijoypur Hills in the Netrokona District of Bangladesh – which is locally called 'white clay'). Before manufacture, green filter kaolin was made in powder form by using hand mortar with pestle then preserved in a dedicator for future use.

2.3. Production and characterization of the water filter

2.3.1 Water Filter Design

For the experiments carried out, the CNF/Kaolin based filter produced in laboratory was manufactured manually, where the shape of the filter was like a cup, with height ~ 8 cm and diameter ~6 cm, with ~3 cm for the upper and lower ends respectively, with a thickness of ~1 cm.

2.3.2 Incorporation of CNFs in the Water Filter

The water filters incorporating the CNFs were made by mixing kaolin (Bijoypur clay) with the prepared CNFs, with the process being as shown in Fig. 2. To create the water filter, bijoypur clay was first powdered and then dipped in distilled water, for 2 hours, to make 'ink' (1g Bijoypur clay to 30 ml water). The prepared 'ink' was then mixed in a 10:1 (10g 'ink' to 1g CNF) ratio with CNF, in a blender for 30 minutes. The mixture was then dried at 40 ºC to form the nano filter material and to stabilize the filter for use in water treatment, it was heated in a furnace, at a temperature of 400 ºC.

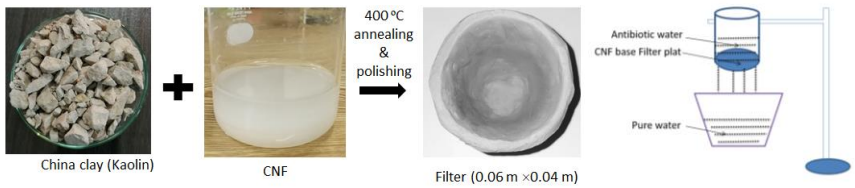

Fig. 2 Illustration of the preparation of the water filter from the CNF samples

2.4 Characterization techniques use for CNF and filter

A Scanning Electron Microscope (SEM) (FESEM, JEOL JSM-7600F) was used to investigate the surface morphology of the plasma-enhanced raw banana fiber, alkali treated fiber (α-Cellulose), bleached fiber, nano-cellulosic fiber and filter. Further, Energy Dispersive X-ray (EDX) analysis was used to investigate the chemical compositions of the filter. In which an accelerating voltage of 5 kV and probe current of ~200 nA were used for this experiment. FTIR spectroscopy (SIMADZU, FMR-$4000 spectrophotometer, Japan) was used to study the inter-molecular and intermolecular interactions. Additionally, a Bruker D8 Advance X-ray Diffractometer with CuK_α radiation of wavelength $\lambda = 1.5418$ Aº allowed XRD measurements

to be carried out in the locked coupled mode, in the 2θ range of 5° to 80° (with a step size 0.02°). The Crystallinity index (CI) of the dried cellulose was determined using the following equation.

$$\mathrm{CI}(\%) = 100 * \frac{A_{\text{crystalline}}}{A_{\text{amorphous}} + A_{\text{crystalline}}}$$

where $A_{amorphous}$ is the area under the amorphous curve, and $A_{crystalline}$ is the area under the sample curve [for definitions of these terms, see the work of Trilokesh et al., 2019]. An X-ray diffraction (XRD) study was performed on the treated fibre, CNF and part of the filter to analyze whether the sample is amorphous or crystalline, doing so in the transmission mode. The thermal properties of the filter materials were also analyzed by the use of a NETZSCH STA 449 F3 Jupiter test instrument. Further, UV-Vis Spectroscopy was used to detect the functional groups, and impurities present, through a qualitative and a quantitative analysis. Finally, studies using a JASCO V-600 spectrophotometer were carried out before and after water purification of the green filter.

3. Analysis and investigation of the CNF and the filter system

3.1 Scanning Electron Microscopy

The surface morphology of the raw, alkali treated, bleached banana fibers and the CNF were studied by using Scanning Electron Microscopy and the morphology of these samples obtained is shown in Fig. 3 (a-d). The SEM micrograph of the raw fiber (Fig. 3 (a)) clearly indicates the intercellular space is filled up by the binder lignin and fatty substances, which hold the unit cells firmly in the fiber. Fig. 3 (b) shows, when compared to the raw banana fiber with 5% NaOH treated fiber, that the fiber surface appears sharpened and impurities were removed with the use of the alkali treatment, showing improved adhesion and revealing micro-fibrils on the fiber topography. This can be described simply as shown in the equation below:

$$\text{Fiber-OH} + \text{NaOH} \Longrightarrow \text{Fiber-O}^{-}\text{Na}^{+} + \text{H}_2\text{O} + [\text{surface impurities}]$$

Fig. 3 (c) shows a SEM picture of the bleached banana fiber, which allows an easy comparison between the raw and bleached fiber surface morphology, where the raw fiber is fully covered by lignin but it is evident that the bleached fibers have a surface which is smoother. The CNF can first be seen in Fig. 3 (d) and, at the magnification used (300X), the nanofiber structure is identifiable; with fiber diameters in the ranges ~300-700 nm. Fig. 3 (d) not only shows the CNF but also that 'honey structures' have appeared – these are essential for producing any types of polymeric nanocomposite, because these structures support interlocking in the filter materials. Thus when such interlocking occurs, very strong bonding is possible, thus to produce a reliable high strength composite.

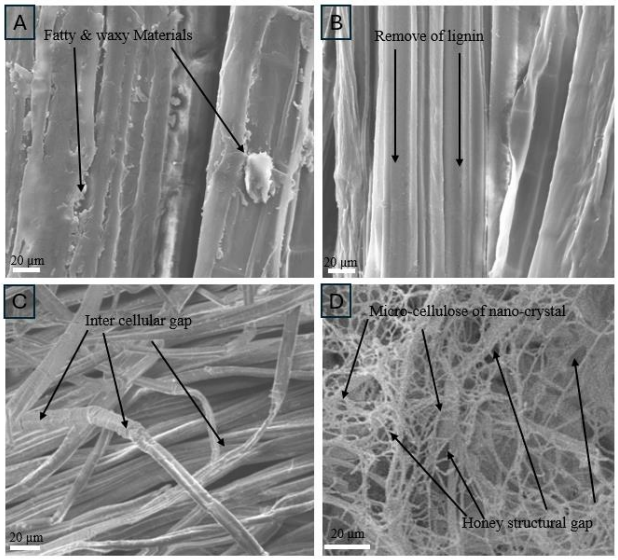

Fig. 3: SEM micrographs of (a) raw banana fibers at a magnification of 1000X, (b) alkali treated banana fibers at a magnification of 1500X, (c) bleached banana fibers at a magnification of 300X and (d) CNF at a magnification of 300X.

Initially, the pure kaolin and green filter surface morphology was investigated by using Scanning Electron Microscopy (SEM), with the result shown in Fig. 4. Here, the kaolin: CNF mixing ratio used was 10:1 in the preparation of the filter. The SEM photograph illustrates the almost homogeneous incorporation of the CNF and the high level of porosity of the filter itself shown in Fig. 4(b), compared to the pure kaolin seen in Fig. 4(a). The CNF used contains hemp fibers, and wood materials (which are cellulose-containing materials which make them promising in terms of the fine structure, high aspect ratio, large specific surface area and good biocompatibility. The CNF has significant physical properties, special surface chemistry, and excellent biological properties which show considerable interest for antibacterial applications (Liu et al., 2015). CNF creates a filter which is more stable in water, of the presence of abundant hydroxyl groups (Aulin et al. 2012).

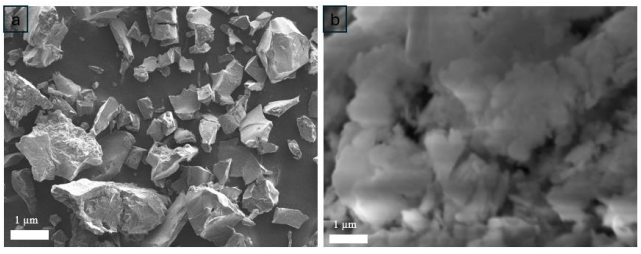

Fig. 4: SEM microscope (a) pure kaolin and (b) Green filter under 10 k magnification.

3.2 Energy Dispersive X-Ray Analysis (EDX)

The result of the EDX analysis, shown in Fig. 5, suggests positively that there is no acidic chemical interaction in the filter. The percentage of the elements shown in the figure indicate that all come from the kaolin and CNF, and those elements have potential antibacterial applications. Kaolin is a clay material which comprises mainly Si, Al and clay mineral basic elements (Deer et al., 1992) – in the EDX carried out, the presence of another element, Ag, was found in the Bangladeshi kaolin sample. The antibacterial activity of Ag nanoparticles is greater than that of Cu and Al nanoparticles (Zia et al., 2018) and thus the presence of Ag in the sample will increase the effectiveness of the filter to remove the antibiotic from the water.

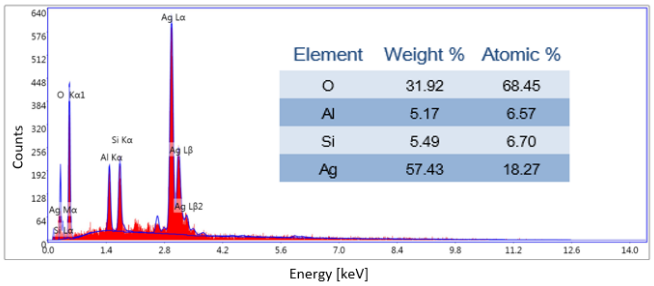

Fig. 5: Results of the EDX analysis of the Green filter, showing its composition

3.3 FTIR analysis

FTIR spectroscopy was chosen to study the intramolecular and intermolecular interactions in polymers (e.g. Lu et al., 2020), and thus in this work raw banana fiber, alkali treated fiber (α-Cellulose), bleached fiber and nano-cellulosic fiber were investigated – the intramolecular and intermolecular hydrogen bonding occurring were investigated by using FTIR spectroscopy (with a SIMADZU, FMR- $4000 spectrophotometer), the results of which are shown in Fig. 6. The characteristic broad feature seen was the absorption of the raw banana fiber (at 3910-3772 cm^{-1}), its presence due to the free –OH group in polymeric association (Dan-asabe et al., 2016). The intensity of the feature at 3323-3237 cm^{-1} due to the hydrogen bonded –OH stretching vibration (vOH) and at 2915-2849 cm^{-1} which arises from the C-H stretching vibration (vCH) from the $–CH_2$ group, due to the cellulose structure, is essentially similar for the three samples investigated (alkali treated, bleached and CNF). The peaks at 1415 cm^{-1} and 1301 cm^{-1} come from the antisymmetric bridge C-O-C stretching vibration (ν-C-O-C-) of the pyranose ring between the cellulose and hemicellulose of the raw banana fiber. The peaks centered on 1456 cm^{-1} and 1240 cm^{-1} indicate the existence of lignin and hemicellulose structures, respectively owing to the asymmetric C-H deformation of the methyl and methylene groups (Zhuang et al., 2020). In the case of the alkali treatment, the presence of an absorption band near 1626 cm^{-1} in the α-Cellulosic fiber IR spectrum was due to >C=O stretching at the carboxylic acid or ester groups, as can be seen from Fig. 6. Lignin showed features at ~1602 cm^{-1}, due to the stretching modes of special types of unsaturation the benzene ring (Dan-asabe et al., 2016). After the alkali treatment, hemicellulose structures were successfully removed, because after the 5%

NaOH treatment applied, only α-Cellulose and lignin exist in the fiber (Cherian et al., 2008). Again, for bleached fiber at ~2367 cm^{-1}, a new peak responsible for C≡C stretching vibration was seen and no peak at ~1400 cm^{-1} – 1500 cm^{-1} was evident, because of the absence of lignin. The FTIR spectra of pure CNF shows two absorption bands between ~2163 and ~2080 cm^{-1} in the CNC spectra which arise due to the C≡C stretching vibration. The presence of an absorption band near ~1635 cm^{-1} in the nano-cellulosic fiber spectrum was due to >C=O stretching, at the carboxylic acid or ester groups, as shown in Fig. 6. The strongest bands across the spectra, seen at ~1157, ~1100 and ~1024 cm^{-1}, can be assigned to –CO stretching and those peaks are blue shifted compared to those seen with raw, alkali and bleaching treatments. The peak seen at ~898 cm^{-1} originated from –OH out-of-plane bending vibrations, which are red shifted compare to others (Dube, 2022, Poyraz et al., 2017). In summary, the significance of this FTIR analysis is that raw banana fibers contained hemicellulose and lignin, which is unstable – but after the treatment both hemicellulose and lignin are removed, this produced the cellulose based CNF, which is more stable and can be used to produce filters which are durable for use.

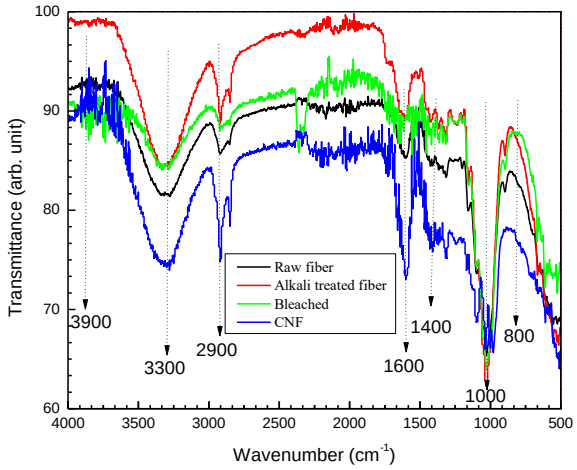

Fig. 6: FTIR analysis of raw, Alkali treated, bleached and CNF banana fiber

Table 1: Functional groups with peak of raw, alkali treated, bleached and nano cellulosic banana fiber

Bond causing the absorption	Raw banana fiber (Peak) cm^{-1}	Alkali treated fiber (Peak) cm^{-1}	Bleached fiber (Peak) cm^{-1}	CNF (Peak) cm^{-1}
Free –OH group	3910-3772		3738	3733
–OH stretching	3323-3237	3325-3246	3435-3289	3347-3281
C−H str (In alkanes)	2915-2849	2922-2844	2926	2894
C≡ C stretching			2367	2163-2080
–CO str (in ester)	1651	1626	1644	1635
C≡C –str (In benzene)	1565	1427		
–C–O–C str	1415			
(C–O) str	1301	1320	1316	1321
(C–O) str	1160-1037	1101-1022	1159-1028	1157-1024
–OH out of plane	871		895	898

The FTIR spectra of the pure kaolin and the kaolin/CNF filter material, designed for use in the filter, are depicted in Figs. 7. The kaolin and kaolin/CNF filter material show bands at 3689 cm^{-1} and 3697 cm^{-1} respectively which are characteristic of inner hydroxyls which hence are not available for interaction with molecules in the filtration process. In the kaolin/CNF filter material, the occurrence of bands 1107 cm^{-1} is similar to what is seen in pure kaolin, i.e. the C–O stretching band. The sharp band at around 902 cm^{-1} and the weak shoulder at 788 cm^{-1} are due to the Al(VI)-OH vibrations for kaolin, and which for the kaolin/CNF filter material can be seen to have shifted 909 cm^{-1}. There is also a weak peak at 785 cm^{-1} for the filter material.

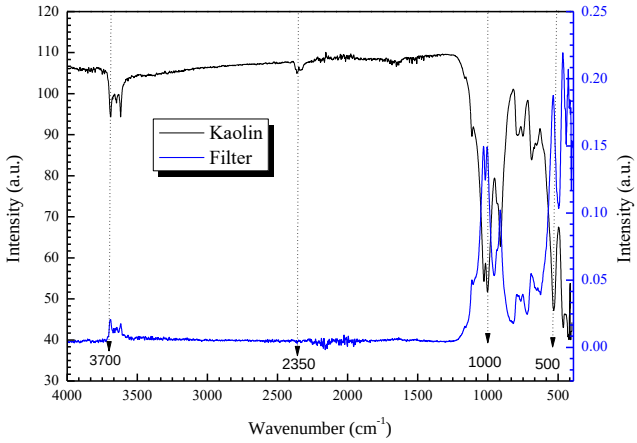

Fig. 7: FTIR analysis of the (pure) kaolin and the kaolin/CNF Filter material

3.4 XRD analysis

The crystallinity of the banana fiber was studied with the aid of X-ray diffraction – and spectra were obtained for different samples as follows: (i) extracted CNF from raw banana fiber, (ii) bleached banana fiber, (iii) alkali treated banana fibers and (iv) raw banana fiber, as shown in Fig. 8(a), where it can be seen that the main diffraction intensity occurred where the angle 2θ = 22°, for each sample. The peak observed close to this point where 2θ = 22.2°, from the raw fiber, has shown very low crystallinity (22%) and this broad feature indicates the amorphous nature of the material. For alkali treated fiber, the crystallinity (51%) increased gradually due to the removal of oil, waxes, lignin and hemi-cellulose and peaks were observed at scattering angles (2θ), at 15° and from 22° and 35° (Meng et al., 2018; French. 2014: Umesh et al., 2021: Isogai et al., 1991: Sunkyu et al., 2010). After bleaching, the peak observed was close to 2θ = 22.4° and the crystallinity was 59%. Using the double acid treatment, the CNF obtained showed a highly crystalline feature with a strong, narrow peak at 2θ = 22.8°. This peak can be attributed to cellulose crystals. It was observed that the CNF had an increased crystallinity from the case of 22% of the raw fibers to the 70% value (Li et al., 2012: Ju et al., 2015: Rico et al., 2020: Yao et al., 2020). The conventional peak deconvolution method was used to fit the amorphous peak position. Although there is no standard model to analyze amorphous cellulose crystallinity, Gauss, Lorentz and Voigt functions can identify the intensity peak position, in fig. 8 (b-e) shows the Lorentz fit for the raw and treated fibers.

As can be seen from Fig. 8(f), the comparative crystallinity of the samples increased after each stage of the series of treatments applied. Cellulose is not comprised of single perfect crystals, because some of hemicelluloses and lignin are contained in them (which are considered as being amorphous, although they are oriented in the same direction as the cellulose fiber) (Wang et al., 2007). Finally, the X-ray diffraction analysis data obtained show that the CNFs have a

higher crystallinity than the raw banana fiber, due to the amorphous hemi-cellulose surrounding in raw fiber. The grain size of the sample can be obtained from the well-known Scherrer equation

$$W = \frac{\lambda}{\beta 1/2 \cos\theta B} \text{.....(1)}$$

where , λ = 1:54 Å is the wavelength of X-ray beam, $\beta_{1/2}$is the full width at half maximum (FWHM) of Bragg'speak from crystalline lattice (in radius) and θ_B is the angular position of Bragg's peaks (in degree).

Table 2 summarizes the data on the structure, obtained from all the peak analyses carried out, showing the values obtained for key parameters: 2θ (degree); FWHM of the peak; d-spacing (Å); *hkl*; Grain Size and %age Crystallinity (French and Santiago Cintrón 2013).

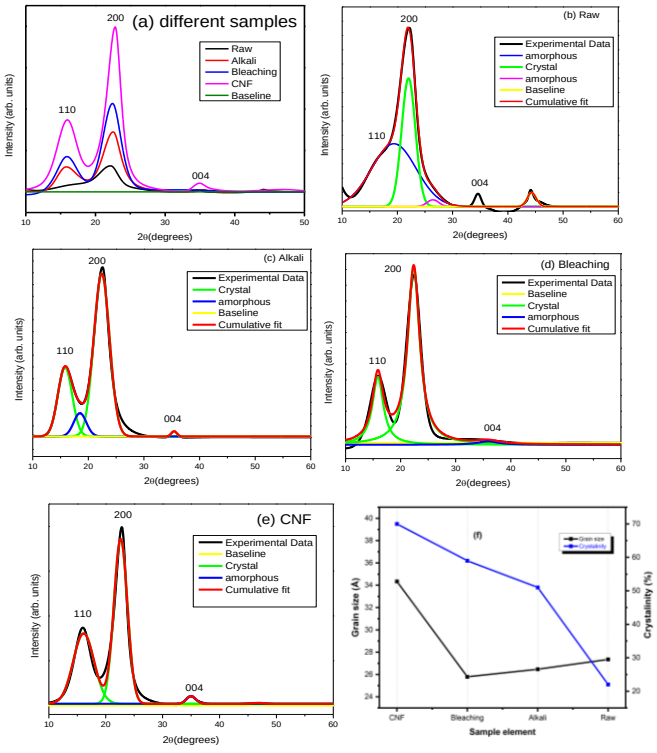

Fig. 8: XRD analysis showing (a) the intensity as a function of the angle, 2θ for different samples (b-e) conventional Lorentz peak fittings, (f) the grain size (nm) and the crystallinity (%) as a function of samples

Table 2 Summary data from the XRD analysis (from Figs. 8)

Name	2θ (degree)	FWHM	d-spacing (Å)	*hkl*	Grain Size (Å)	Crystallinity, %
CNF	15.90	3.17	5.57	110	34.34	70
	22.81	2.36	3.89	200		
	34.94	2.44	2.56	004		
Bleaching	15.87	3.82	5.58	110	25.79	59
	22.47	3.14	3.96	200		
Alkali	15.8	3.80	5.60	110	26.47	51
	22.55	3.06	3.94	200		
	35.35	1.43	2.53	004		
Raw	22.22	2.96	3.99	200	27.35	22
	34.57	2.61	2.59	004		

X-ray diffraction analysis has been used to make a comparison between the kaolin and the kaolin/CNF filter material. The intensity of the signal received from the kaolin/CNF filter material decreases with increasing wt% of CNF, as can be seen in Fig. 9 which illustrates the differences in the peak intensity and how it changes for the two samples. The XRD analysis of kaolin is compared with the data in the literature (Dewi et al., 2018). Table 3 also indicates the average grain size is reduced when the kaolin sample is converted to the kaolin/CNF filter material.

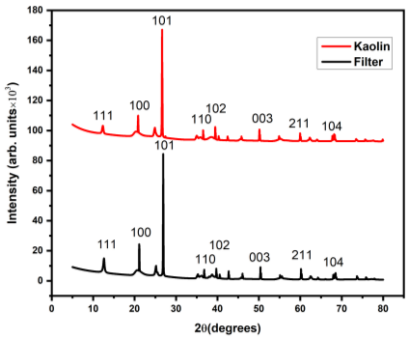

Fig. 9: XRD analysis for comparing the pure kaolin sample (labelled Kaolin) and the kaolin/CNF filter material (labelled Filter)

401 Table 3 Results of the XRD analysis comparing the pure kaolin sample and the kaolin/CNF
402 filter material

Name	2 theta (degree)	FWHM	d-spacing (angstrom)	hkl	Average Grain Size
Pure Kaolin	12.59	0.36	7.02	111	839.27
	21.60	0.07	4.21	100	
	26.89	0.06	3.32	101	
	38.69	0.53	2.57	110	
	39.72	0.067	2.27	102	
	50.37	0.075	1.81	003	
	60.18	0.08	1.54	211	
	67.69	0.08	1.28	104	
Kaolin/CNF Filter material	12.32	0.36	7.18	111	764.01
	20.80	0.11	4.27	100	
	26.64	0.09	3.34	101	
	38.50	1.39	2.34	110	
	39.45	0.07	2.28	102	
	50.14	0.09	1.82	003	
	59.96	0.09	1.54	211	
	67.47	0.12	1.29	104	

403

404 3.5 Thermal analysis of the fibers

405 The thermal behavior of the raw fiber, the alkali treated fiber, the bleached and the CNF fibre,
406 in a N_2 environment, has been investigated using Thermo-Gravimetric Analysis (TGA) and
407 Differential Thermal Analysis (DTA) and the data obtained are shown in Fig. 10 (a and b). The
408 thermal degradation of the fiber investigated over the temperature range from ~25–600°C (in
409 the N_2 environment) was studied with a continuous heating rate of 10°C/min being applied.
410 An initial weight loss of ~11 % over the temperature range ~50-240°C was observed, due to
411 the evaporation of bound moisture from the raw fiber (the moisture range for banana fiber is
412 known to be ~11-15%) (Deepa et al., 2011), likely due to water molecules being released. The

second (and dominant) weight loss was observed at temperatures ~240-400°C, leading to the formation of volatile chemicals of low molecular weight, owing to the pyrolysis of the banana fiber. All these stages of degradation occurred due to hemicellulose, cellulose, and lignin, respectively as generally, thermal degradation of banana involves dehydration, depolymerization and decomposition of glycosyl-units and then the formation of a chaffed residue.

The graphs obtained following the four stages of treatment are shown in Fig. 10 (a) using TGA for (1) the raw, (2) alkali, (3) bleached and (4) cellulose banana, showing residues of 0%, 4%, 2% and 6% respectively after heating to 600°C. The temperature showing the onset of the degradation decreased gradually from 300°C to 280 °C, confirming the removal of the hemicellulose and the lignin, where these results suggested that the chemical modification decreased the thermal stability of the raw banana fiber. For CNF, in the cellulose pyrolysis mechanism, initially the moisture inside the cellulose evaporates in the first stage of heating and the thermal decomposition of cellulose components begins with increasing pyrolysis temperature.

The DTA data in Fig. 10 (b) show one sharp endothermic peak at 298 ºC in the case of CNF and three endothermic peaks at 260, 230, and 240 ºC in the cases of (1) raw, (2) alkali treated and (3) bleaching of the banana fiber. Fig. 10 (b) also shows that the DAT curves are endothermic, so there are no chemical interactions and only physical changes present. In (4), for CNF, the shape of the graph shows an endothermic peak, indicating high crystallanity (which is also supported by the XRD analysis). From these DTA data, by comparison to (1) raw fiber, (4) CNF is the more thermally stable and its characteristic transition or reaction temperature can also accurately be determined. Table 4 show weight loss calculation for different samples from the TG-DTA carried out.

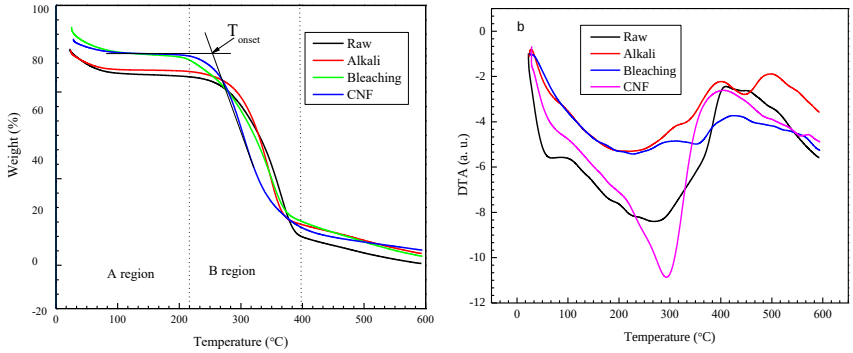

Fig. 10: (a) TGA and (b) DTA thermographs of (1) raw banana fiber; (2) alkali treated banana fibers; (3) after bleaching of the banana fiber and (4) extracted CNF from raw banana fiber in the N_2 environment used

Table 4 Weight loss calculation for different samples from TG-DTA

Sample Name	Temperature Region (0-240 °C) Weight loss (%)	Temperature Region (240-400 °C) Weight loss (%)	T_{onset} (°C)	$T_{50\%}$ (°C)
(1) Raw	11	78	300	376
(2) Alkali	09	72	298	377
(3)Bleaching	5	80	272	360
(4) CNF	7	72	280	345

4. Discussion of Filter Operation and UV-Vis Spectral analysis and mechanism /Performance of the water filter, obtained using UV-Vis Spectral analysis

In this test, a standard antibiotic solution was prepared by using a simple mix of a number of widely used and easily available antibiotics. Thus ciprocin 500, Klarix 500, Eromycin Ds 500, Filmet 400 and Cotrim Ds antibiotic tablets were chosen and purchased and used as obtained from the local market (in Bangladesh), as a source of a familiar group of antibiotics, Ciprofloxacin, Clarithromycin, Erythromycin, Metronidazole, Sulfamethoxazole and Trimethoprim. These were removed from the packaging and crushed using a pestle and mortar. The powders thus formed from each of the samples were used to make a 1mM antibiotic solution in distilled water.

Prior to their being passed through the filter, these solutions were examined using UV-Vis spectroscopy. Given the relatively high concentrations seen, the Ciprofloxacin, Metronidazole, Sulfamethoxazole and Trimethoprim antibiotic solutions were diluted with distilled water (X30 for Ciprofloxacin, X20 for Metronidazole, Sulfamethoxazole and Trimethoprim) as the UV-Vis absorption was otherwise very high. In this way, the intensity of the absorption for each of the antibiotics was approximately at the same level over the 200 – 400 nm regions. Fig. 11 shows the absorption spectra of all the individual antibiotic solutions examined and a similar pattern of strong absorption in the 200 – 400 nm region can be seen, this 'tailing off' beyond 400 nm in the visible region. Table 5 shows the concentration of antibiotic for UV-Vis Spectral analysis.

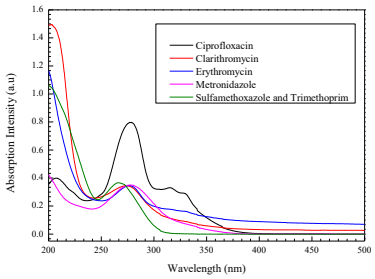

Fig. 11: UV-Vis spectra of the individual antibiotic solutions listed

In order to evaluate the performance of the filter, a solution containing all the antibiotic samples (which were brought together in equal amounts to create a single sample) then was subjected to filtration using the kaolin/CNF filter material. Two solutions were made up (a) one of 6 x 5 ml samples, containing 5 ml of each of the antibiotics mentioned and (b) one of 6 x 10 ml samples, containing 10 ml of each of the antibiotic mixture.

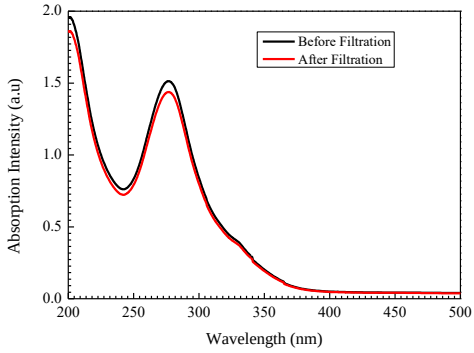

Fig. 12: Before and after filtration for the sample of all antibiotic solutions using the filter made by only using kaolin clay

Fig. 12 shown the UV-Vis spectra in the region 200 – 500 nm for the situation before the filtration of the solution – i.e. it was passed through the only kaolin clay (only) filter and in this case there was no CNFs in the filter. It is clear from the results of the experiment shown that only a very small amount of antibiotics was removed from the aqueous antibiotic mixture solution. All the filtration processes were tested five times to identify the saturation point. The conclusion is that the influence of the kaolin alone on the solution containing the antibiotic mixture is low.

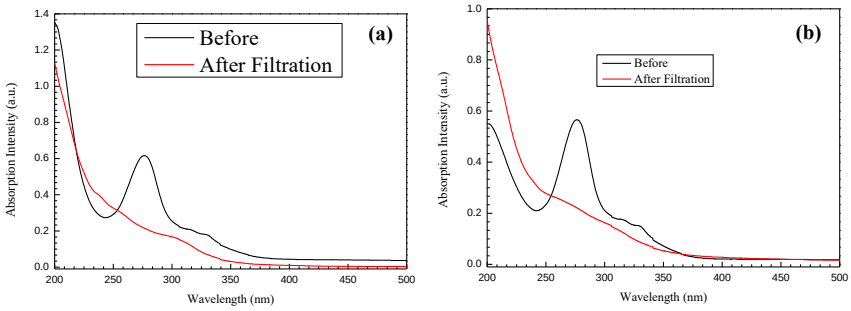

Fig. 13 : Before and after filtration (a) for the solution sample of all the antibiotics in the mixture, each at 5ml and (b) for the solution sample of all the antibiotics, each at 10ml using the filter developed

UV-Vis spectra in the region 200 – 500 nm were taken both before the solution was passed through the filter material, and after, for both samples (a) and (b), as shown in Fig. 13. Visual inspection of the graphs shows the efficacy of the filter in the removal of the antibiotics, with the major reduction of the peak at ~280 nm seen. This is a convenient 'marker wavelength' for the filter, as both the UV-Vis spectrum of pure distilled water in that spectral region is negligible (György et al., 2013) and all the antibiotics show a significant peak at that wavelength band. Thus using this peak, with the 6 x 5ml sample, the filter caused a drop in the peak from 0.60 ± 0.02 to 0.22 ± 0.02 au; with the 6 x 10 ml sample, this drop was from 0.58 ± 0.02 to 0.22 ± 0.02 au (all with reference to a background from distilled water that is 0.0 ± 0.2 au). On that basis, a 'figure of merit' for the filter for the typical antibiotic mixture used of 2.7 ± 0.1 can be derived for each pass through the filter. Multiple passes of the liquid sample can be used, thereby increasing the degree of filtration of this simple and inexpensive device.

Table 5 Concentration of antibiotic for UV-Vis Spectral analysis

Antibiotic name	Concentrations (mM)
Ciprofloxacin	0.03
Clarithromycin	1.00
Erythromycin	1.00
Metronidazole	0.05
Sulfamethoxazole	0.05
Trimethoprim	0.05

Antibiotics, which end up in waste water, are of growing concern, as they can accumulate in aquatic organisms (Le-Minh et al. 2010). Antibiotics in water display cationic, anionic, or non-ionic properties. There are extensive reports on the use of nanocellulose as drug carriers, but studies on the adsorption of drugs onto nanocellulose are sparse. Jackson et al. (Jackson et al. 2011) first confirmed the capacity of sulfated nanocellulose to adsorb ionized drugs. The interactions between the antibiotic solution and the cellulose nanofiber have been crucially important for human beings and the environment. Cellulose nanofibers (CNFs) used here were simply prepared by a double hydrolysis of sulfuric acid treatment therefore the adsorption capacity of CNF is high due to the sulfate ($–SO_3^-$) functional groups on the surface of CNF (Liu et al. 2014). CNFs can adsorb cations and heavy metals from water solution, and kaolin have cations like Cu, Ag and Al which can block anions from solutions. The adsorption behavior depends on pH of the solution, and near neutral pH shows the best adsorption performance. The pH was kept at a value of 6.5 and this filter adsorbs the cationic and anionic of antibiotics solutions.

Discussion and Conclusions

The CNFs discussed in this work have been successfully synthesized through a two-step process, from agricultural waste banana fiber. Given this very productive use of an otherwise waste material, this has been shown to be very promising as a nanocomposite with reinforcing materials. An intensive and multi-facetted analysis of the material created was undertaken, as summarized below. The surface morphology was shown to be a nano-cellulose arrangement,

the partial size was 300-700 nm, and the surface of the CNF comprises a honeycomb structure, which helps to produce a very strong composite with polymeric materials. The FTIR analysis results obtained in this work show the structural changes in the process of converting the raw fiber to CNF, which then enables the production of the cellulose nano fiber. The crystallinity increase from 22% to 70%, from raw fiber to CNF, is revealed by the XRD analysis carried out, a result which is consistent with that from the FTIR analysis. The thermal degradation behavior was shown by the results of the TGA carried out and the CNF used here was shown to be more thermally stable, compared to raw banana fiber. The DTA results also support the results of the XRD analysis, showing the change in the crystallinity index, this being seen to increase in the case of the CNF.

Finally, with the outcome of these evaluations of the material, it was used to create an inexpensive and easy-to-fabricate biodegradable water filter, using readily available kaolin clay combined with the CNF and it tested for its efficacy to remove antibiotics from the wastewater. The water filter designed and evaluated in this work successfully removed > 90% of the sample antibiotic mixture from the waste water. This is a very satisfactory result and shows that an inexpensive and locally-produced filter can readily be produced from what is otherwise a waste material using a simple processing technique. Therefore, as the cellulose nano fiber is bio-degradable and eco-friendly, it is an excellent material to use here as in antibacterial application.

Acknowledgements: Authors would like to thank the Global Challenges Research Fund allocation authority for their financial support. The authors would like to express their appreciation to the Islamic University Kushtia, Bangladesh, Bangladesh University of Engineering and Technology (BUET), and Bangladesh Council of Scientific and Industrial Research (BCSIR), Dhaka, Bangladesh for providing the support needed to carry out this research.

Funding: This work was supported by the financial support of the Global Challenges Research Fund (GCRF) United Kingdom (48314AY).

Declaration of interests

The authors declare that they have no known competing financial interests or personal relationships that could have appeared to influence the work reported in this paper.

Author Contributions Statement

Conceptualization, M.M.A, M. J.S. & S. N; methodology, S,N. and K. G.; data analysis, M.M.A. , M.J.I, S. N.; investigation, M.J.I., M.M.A. & S. N writing—original draft preparation, S.N.& K.G,; writing—review and editing, M.M.A, S.N. K.G. and C,H,; supervision, project administration, and funding acquisition, All authors have read and agreed to the published version of the manuscript.

References

An Y , Li F, Di Y, Zhang X , Lu J, Wang L, Yan Z, Wang W, Liu M, Fei P (2024) Hydrophobic Modification of Cellulose Acetate and Its Application in the Field of Water Treatment: A Review. Molecules. 30;29(21):5127. doi: 10.3390/molecules29215127.

Aulin C, Salazar-Alvarez G, Lindstrom T, (2012) High strength, flexible and transparent nanofibrillated cellulose–nanoclay biohybrid films with tunable oxygen and water vapor. permeability Nanoscale 4:6622-6628. https://doi.org/10.1039/C2NR31726E

Chee-Sanford JC, Aminov RI, Krapac IJ et al (2001) Occurrence and Diversity of Tetracycline Resistance Genes in Lagoons and Groundwater Underlying Two Swine Production Facilities. Appl Environ Microbiol 67(4): 1494–1502. https://doi.org/10.1128/AEM.67.4.1494-1502.2001

Cherian BM, Pothan LA, et al (2008) A Novel Method for the Synthesis of Cellulose Nanofibril Whiskers from Banana Fibers and Characterization. J Agric Food Chem 56(14): 5617–5627. https://doi.org/10.1021/jf8003674

Dan-asabe B et al (2016) Mechanical, Spectroscopic and Micro-structural Characterization of Banana Particulate Reinforced PVC Composite as Piping Material. Journal of Tribology in Industry. 38(2):255-267. doaj.org/article/1881a705951d4bb793dc4ff0fd0aadd8

Deepa B. et al (2011) Structure, morphology and thermal characteristics of banana nano fibers obtained by steam explosion. Bioresource Technology 102:1988-1997. https://doi.org/10.1016/j.biortech.2010.09.030

Deer WA, Howie RA, Zussman J (1992) An Introduction to the Rock-forming Minerals (2nd Ed.). Harlow, Essex, England: Longman Scientific & Technical; New York, NY: Wiley. ISBN 9780470218099. DOI:https://doi.org/10.1180/DHZ

Dewi, R; Agusnar, H; Alfian, Z; Tamrin, (2018) *Characterization of technical kaolin using XRF, SEM, XRD, FTIR and its potentials as industrial raw materials. Journal of Physics: Conference Series, 1116(), 042010–*. doi:10.1088/1742-6596/1116/4/042010

Drinan, J.E., (2001). Water and Wastewater Treatment: A Guide for the Nonengineering Professional; CRC Press LLC: Florida. DOI: https://doi.org/10.1201/b12354

590 Dube, A. M. 2022. “Isolation and Characterization of Cellulose Nanocrystals from Ensete
591 Ventricosum Pseudo-Stem Fiber Using Acid Hydrolysis.” Biomass Conversion and
592 Biorefinery. (123456789). Springer Berlin Heidelberg. doi. https://doi.org/10.1007/s13399-
593 022-02987-z

594 French, AD. (2014). *Idealized powder diffraction patterns for cellulose polymorphs.*
595 *Cellulose, 21(2), 885–896.* doi:10.1007/s10570-013-0030-4

596 French AD, Santiago Cintrónel M (2013), Cellulose polymorphy, crystallite size, and the
597 Segal Crystallinity Index. Cellulose, 20(1), 583–588. doi:10.1007/s10570-012-9833-y

598 GilPavas E, Dobrosz-Gómez I, Gómez-García MÁ (2017) Coagulation-flocculation
599 sequential with Fenton or Photo-Fenton processes as an alternative for the industrial textile
600 wastewater treatment. J Environ Manage 191:189–197. https://doi:
601 10.1016/j.jenvman.2017.01.015

602 Gupta SS, Bhattacharyya KG (2008) Immobilization of Pb (II), Cd(II) and Ni(II) ions on
603 kaolinite and montmorillonite surfaces from aqueous medium. J. Environ. Manage. 87:46–
604 58. https://doi: 10.1016/j.jenvman.2007.01.048

605 György E, et al (2013) Processing and immobilization of chondroitin-4-sulphate by UV laser
606 radiation. Colloids and Surfaces B: Biointerfaces. 104(), 169–173. https:// doi:
607 10.1016/j.colsurfb.2012.11.044

608 Herbert RM (1954) Textile Fibres, Their Physical, Microscopy and Mechanical Properties.
609 Chapman and Hall, London. DOI: 10.1126/science.120.3119.566.a

610 Hani Nasser Abdelhamid (2024) Nanocellulose-Based Materials for Water Pollutant
611 Removal: A Review. International Journal of Molecular Sciences. 25(15), 8529.
612 https://doi.org/10.3390/ijms25158529

613 Hokkanen S, Bhatnagar A, Sillanpää M (2016) A review on modification methods to
614 cellulose-based adsorbents to improve adsorption capacity. Water Research 91:156-173.
615 https://doi.org/10.1016/j.watres.2016.01.008

Islam, M. J., Rahman, M. J., & Mieno, T. 2020. Safely functionalized carbon nanotube–coated jute fibers for advanced technology. J of Adv Compos and Hyb Mater 3, 285–293. https://doi: 10.1007/s42114-020-00160-6

Islam, M. J., Kamaruzzaman, Rahman, M. J., Alam, M. M., 2021. Carbon nanotube reinforced natural fibers for biodegradable Nanocomposites. Am j polym sci technol 7(4), 73-79. https://doi.org/10.4236/msa.2021.1212038

Imam MZ and Akter S (2011) Musa paradisiaca L. and Musa sapientum L.: A Phytochemical and Pharmacological Review. J Appl Pharm 01 (05):14-20.

Isogai A, Atalla RH (1991) Amorphous Celluloses Stable in Aqueous Media: Regeneration from SO,-Amine Solvent Systems. J Polym Sci A Polym Chem 29: 113-119. https://doi.org/10.1002/pola.1991.080290113

Jackson JK, Letchfor K et al (2011) The use of nanocrystalline cellulose for the binding and controlled release of drugs. Int. J. Nanomed., 6:321–330. https://doi: 10.2147/IJN.S16749

Ju X, Bowden M, Brown EE, Zhang X (2015) An improved X-ray diffraction method for cellulose crystallinity measurement Carbohydrate Polymers Volume 123:476481. https://doi.org/0ee4431e4932fb1a8e360153c0088156

Kamble P, Newale K, Kanthak R, Patil P, Gunjavate P, (2018) Effect of alkali treated banana fibers on tensile properties of bio-composite material. Int. J. of Engg. and Tech. Vol. 5, Issue:10. https://doi.org/10.1177/1528083717714479

Lakretz A, Elifantz H, Kviatkovski I, Eshel G, Mamane H (2014) Automatic microfiber filtration (AMF) of surface water: Impact on water quality and biofouling evolution. Water Research, 48:592–604. https://doi.org/10.1016/j.watres.2013.10.018

Le-Minh N, Khan SJ, Drewes JE, Stuetz RM (2010) Fate of antibiotics during municipal water recycling treatment processes. Water Research, 44:4295–4323. https://doi.org/10.1016/j.watres.2010.06.020

Li R, Zhang L, Xu M (2012) Novel regenerated cellulose films prepared by coagulating with water: Structure and properties. 87(1):95 100. https://doi.org/10.1016/j.carbpol.2011.07.023

643 Liu K, Chen L, Huang L et al (2015) Enhancing antibacterium and strength of cellulosic
644 paper by coating triclosan-loaded nanofibrillated cellulose (NFC). Carbohydrate Polymers,
645 117:996–1001. https://doi.org/10.1016/j.carbpol.2014.10.014

646 Liu P, Sehaqui H et al (2014) Cellulose and chitin nanomaterials for capturing silver ions
647 (Ag^+) from water via surface adsorption. Cellulose 21:449–
648 461. https://doi.org/10.1007/s10570-013-0139-5

649 Lu H, Shinzawa H, Kazarian S.G (2020) Intermolecular Interactions in the Polymer Blends
650 Under High-Pressure CO_2 Studied Using Two-Dimensional Correlation Analysis and Two-
651 Dimensional Disrelation Mapping. Appl Spectrosc 75(3):250
652 258. https://doi.org/10.1177/0003702820978473

653 Mahjoub R, Yatim JM et al (2014) Tensile properties of kenaf fiber due to various conditions
654 of chemical fiber surface modifications. Constr Build Mater 55:103–113.
655 https://doi.org/10.1016/j.conbuildmat.2014.01.036

656 Mateo S. et al (2021) Nanocellulose from Agricultural Wastes: Products and Applications—
657 A Review. *Processes*. *9*(9):1594. https://doi.org/10.3390/pr9091594

658 Meng F, Wang G, et al (2018) Preparation and characterization of cellulose nanofibers and
659 nanocrystals from liquefied banana pseudo-stem residue. Composites Part B: Engineering
660 160:341-347. https://doi.org/10.1016/j.compositesb.2018.08.048

661 Percot A, Viton C, Domard A (2003) Optimization of Chitin Extraction from Shrimp Shells.
662 Biomacromolecules. 4(1):12–18. https://doi: 10.1021/bm025602k

663 Poyraz B, Tozluoglu A, Candan Z, Demir A, Yavuz M (2017) Influence of PVA and silica
664 on chemical, thermo-mechanical and electrical properties of Celluclast-treated
665 nanofibrillated cellulose composites. Int J Biol Macromol. 104 (Pt A)
666 DOI: 10.1016/j.ijbiomac.2017.06.018

667 Radoor S, Karayil J, Jayakumar A, Kandel D.R,Kim J.T, Suchart Siengchin S, Lee J (2024)
668 Recent advances in cellulose- and alginate-based hydrogels for water and wastewater
669 treatment: A review. Carbohydrate Polymers. 323(1)121339.
670 https://doi.org/10.1016/j.carbpol.2023.121339

671 Rahman MM, Maniruzzaman M, Islam MR, Rahman M S (2018) Synthesis of Nano-
672 Cellulose from Okra Fibre and FTIR as Well as Morphological Studies on It. Am j polym sci
673 technol 4(2):42-52. https://doi:10.11648/J.AJPST.20180402.11

674 Rico del Cerro DR, Koso TV, Kakko T, King AWT, Kilpeläinen (2020) Crystallinity
675 reduction and enhancement in the chemical reactivity of cellulose by non-dissolving
676 pretreatment with tetrabutylphosphonium acetate. Cellulose. https://doi.org/10.1007/s10570-
677 020-03044-6

678 Sharma R, Nath P.C, Mohanta Y.K., Bhunia B, Mishra B, Sharma M,Suri S, Bhaswant N
679 ayak P. K., Sridhar K (2024) Recent advances in cellulose-based sustainable materials for
680 wastewater treatment: An overview. International Journal of Biological Macromolecules.
681 256(2), 128517. https://doi.org/10.1016/j.ijbiomac.2023.128517

682 Sunkyu Park; John O Baker; Michael E Himmel; Philip A Parilla; David K Johnson
683 (2010). Cellulose crystallinity index: measurement techniques and their impact on
684 interpreting cellulase performance. , 3(1). https://doi.org/10.1186/1754-6834-3-10

685 Teh CY, Budiman PM, Shak KPY, Wu TY (2016) Recent advancement of coagulation-
686 flocculation and its application in wastewater treatment. Ind Eng Chem Res 55(16):4363–
687 4389. https://doi.org/10.1021/acs.iecr.5b04703

688 Trache D, Tarchoun AF, Derradji M et al (2020) Nanocellulose: From Fundamentals to
689 Advanced Applications. Frnt Chem 8:392. https://doi.org/10.3389/fchem.2020.00392

690 Trilokesh, C.; Uppuluri, Kiran Babu (2019). Isolation and characterization of cellulose
691 nanocrystals from jackfruit peel. Scientific Reports, 9(1), 16709–. doi:10.1038/s41598-019-
692 53412-x

693 Umesh P. Agarwal, Sally A. Ralph, Carlos Baez;Richard S. Reiner (2021) Contributions of
694 Crystalline and Noncrystalline Cellulose Can Occur in the Same Spectral Regions: Evidence
695 Based on Raman and IR and Its Implication for Crystallinity Measurements.
696 Biomacromolecules, 22:1357-1373. https://doi:10.1021/acs.biomac.0c01389

697 Wang B, Sain M, Oksman K (2007) Study of Structural Morphology of Hemp Fiber from the
698 Micro to the Nanoscale. Applied Composite Materials. 14(2):89–
699 103. http://dx.doi.org/10.1007/s10443-006-9032-9

700 Wang S, Li X, Zhao H, Quan X, Chen S, Yu H (2018) Enhanced adsorption of ionizable
701 antibiotics on activated carbon fiber under electrochemical assistance in continuous-flow
702 modes. Water Research 134:162-169. https://doi.org/10.1016/j.watres.2018.01.068

703 Wan K, Guo L et al (2021) Accumulation of antibiotic resistance genes in full-scale drinking
704 water biological activated carbon (BAC) filters during backwash cycles. Water Research
705 190(5):116744. http://dx.doi.org/10.1016/j.watres.2020.116744

706 Yao W, Weng Y, Catchmark J (2020) Improved cellulose X-Ray diffraction analysis using
707 Fourier series modeling. Cellulose 27:5563–5579. https://doi.org/10.1007/s10570-020-
708 03177-8

709 Zia R, Riaz M, Farooq N, Qamar A, Anjum S (2018) Antibacterial activity of Ag and Cu
710 nanoparticles synthesized by chemical reduction method: a comparative analysis. Materials
711 Research Express. 5(7):075012. https://doi.org/10.1088/2053-1591/aacf70

712 Zhuang J, Li M, Pu Y, Ragauskas AJ, Yoo CG (2020) Observation of Potential Contaminants
713 in Processed Biomass Using Fourier Transform Infrared Spectroscopy. Applied Sciences.
714 10(12):4345. https://doi.org/10.3390/app10124345